

Propagator Resolved Transverse Relaxation Exchange Spectroscopy

K.E. Washburn^{a,c}, C.H. Arns^b, P.T. Callaghan^a

^a*The MacDiarmid Institute, Victoria University of Wellington, Wellington, New Zealand*

^b*Department of Applied Mathematics, Australian National University, Canberra, Australia*

^c*ResLab, Reservoir Laboratories AS, Trondheim, Norway*

Abstract. We use the propagator resolved transverse relaxation exchange technique to look at the movement of fluid in three different types of rock samples. The two pore model previously used to fit molecular exchange simulations to the experimental data is expanded to accommodate the three site exchange seen in two of the samples. Estimated values for pore space characteristics from the simulations were compared to values calculated from X-Ray CT data of the samples. While discrepancies exist between the NMR and X-Ray CT results, the molecular exchange behavior estimated from the three samples reflects well with their morphology.

Keywords: T₂-T₂ exchange, propagator, pore, rocks.

PACS: 82.56.Fk, 87.64.kj, 78.55.Mb, 81.05.Rm

INTRODUCTION

Characterization of the behavior of fluid in a porous material is of interest to a wide variety of fields such as oil recovery, chemical engineering, and medicine. Nuclear magnetic resonance (NMR) has been widely used to this aim, as it is non-invasive and can be performed on opaque samples. To help observe the movement of fluid molecules between differing environments, researchers have used transverse relaxation exchange experiments^{1,2}. This technique correlates the T₂ times of spin-bearing fluid molecules separated by a mixing time. When a two dimensional inverse Laplace transform is applied to the data, a spectrum similar in form to Fourier exchange experiments is produced. Molecules that are in their original environment appear along the diagonal while molecules that have changed environment will appear as cross peaks. The technique was limited however, in that it cannot distinguish signal of spin-bearing molecules that have exchanged between pores of similar size from molecules that have remained in their original environment. To provide more information about the fluid movement, a third, propagator dimension was added to the transverse relaxation exchange experiment³, so that the distance that the fluid molecules move during the mixing time can be measured. These experiments were performed on tight-packed quartz sand. By fitting to the theory, we are able to estimate parameters such as pore size, inter-pore spacing, pore characteristic times, and tortuosity. In this paper, we examine more samples to see how the exchange behaviour compares with the different sample morphology. We also modify our simulations to account for three site exchange.

EXPERIMENTAL

To expand upon the previous propagator resolved transverse relaxation exchange work³, we performed the experiments on two additional samples, Fontainebleau sandstone and Mt. Gambier limestone. The three different samples show a range of morphology. Properties of the three samples were calculated from X-Ray CT images⁴, shown in Fig. 1. Fontainebleau is a very clean, homogenous sandstone and our sample had approximately 15% porosity. The pore sizes range from approximately 20 μm to 100 μm in diameter. The average inter-pore spacing is approximately 100 μm with a spread of about 40 μm. The tortuosity of the Fontainebleau ranged from around 3 to

6. Mt Gambier is a limestone containing a wide range of pore sizes with about 50% porosity. The pore sizes ranged from approximately 10 μm to 200 μm in diameter. The average inter-pore spacing is approximately 140 μm with a spread of about 90 μm . The tortuosity of the Mt. Gambier ranged from around 2 to 6. The tight-packed quartz sand was in between with 35% porosity. The pore sizes ranged from approximately 20 μm to 120 μm in diameter. The average inter-pore spacing is approximately 200 μm with a spread of about 100 μm . The tortuosity of the sand sample ranged from 1.4 to 2.2.

All three samples were saturated with distilled water. The experiments were performed with mixing times from 50 ms to 550 ms in 50 ms intervals. A fixed echo spacing of 150 μs was used to minimize the influence of internal gradients. After experimentation, the data was zero filled along the diffusion axis and Fourier transformed to produce the average propagator. Planes of T_2 - T_2 exchange data were extracted from along the propagator and transformed using a 2D inverse Laplace⁵ transform. The peak intensities were integrated and plotted as a function of mixing time and displacement; examples of a diagonal and a cross peak are shown in Fig. 2 from the quartz sand sample.

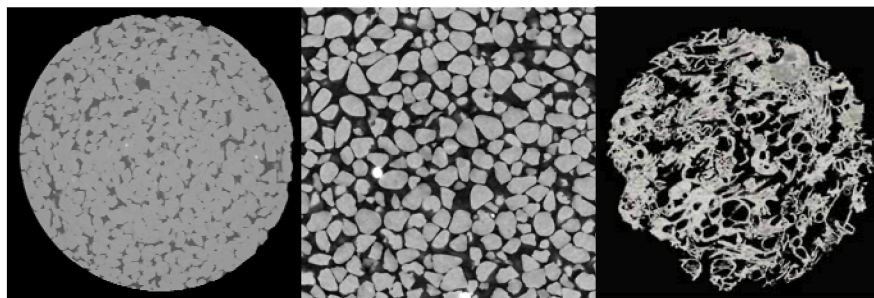


FIGURE 1. micro X-Ray CT tomographs of (a) Fontainebleau (b) tight-packed quartz sand (c) Mt. Gambier limestone

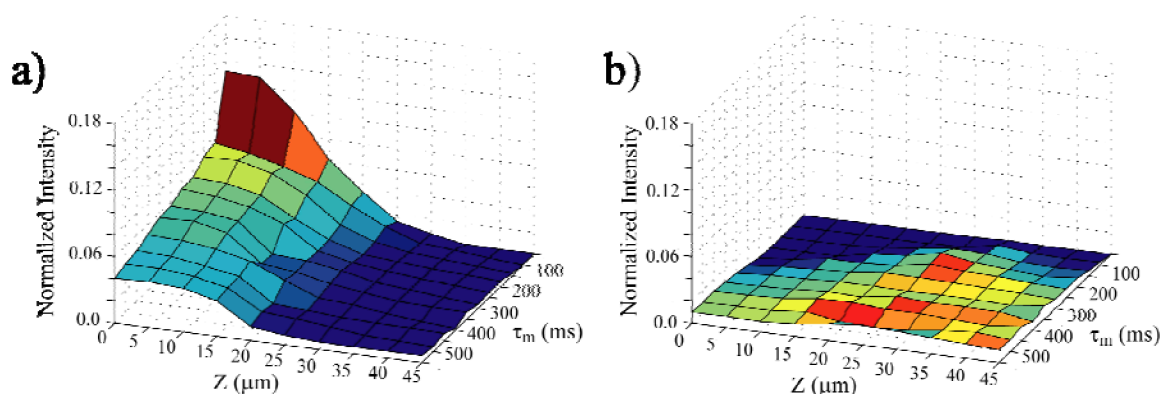


FIGURE 2. Experimental peak intensities for the quartz sand as a function of mixing time, τ_m (ms), and displacement, Z (μm), for (a) a diagonal peak (b) a cross peak. The minimum to maximum intensity in the plot is depicted by the color range from blue to red.

ANALYSIS AND DISCUSSION

Simulated peak intensities calculated from theory are fitted to the experimental results by optimisation of several pore characteristics. Previously, in calculation of our simulated fits we had disregarded the smallest peak in the sand sample, as it only comprised a small percentage of the total signal intensity. With our limestone sample, the smallest peak in the spectrum is not weak enough that we can disregard it. To account for this, we modify the two pore exchange simulations for a three site exchange. The Fontainebleau sample only produced two peaks in the spectra, so the two-pore model was applied to it.

Fig. 3 shows the simulated peak intensity fit to the experimental peak intensities shown in Fig. 2. There continues to be significant discrepancy between the simulated NMR and experimental NMR peak intensities for the cross peaks. This most likely stems from resolution issues of the inverse Laplace transform. Often weaker peaks are not distinguished in the presence of much stronger peaks. Therefore, until the weaker peak has a large enough

intensity relative to the stronger peak, it will not be resolved. This may explain the weak intensities seen at short displacements and mixing times despite theory predicting stronger intensity. The Mt. Gambier, which shows the most exchange, has experimental cross peak intensities that best resemble the predicted theory, while the Fontainebleau, with its meager exchange, shows the most deviation.

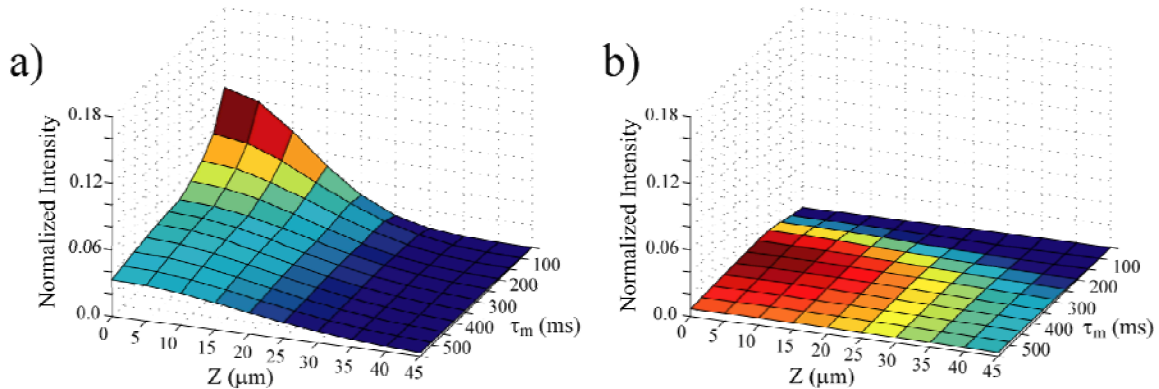


FIGURE 3. Simulated peak intensities for the quartz sand as a function of mixing time, τ_m (ms), and displacement, Z (μm), for (a) a diagonal peak (b) a cross peak. The minimum to maximum intensity in the plot is depicted by the color range from blue to red.

All three samples produce pore radii consistent with the calculated values from X-Ray CT. We see better agreement with the inter-pore spacing in the Fontainebleau and Mt. Gambier than we do in the sand sample. However, this is most likely resulting from the fact that the two samples appear to have smaller spacings than the tight-packed quartz sand so we can better probe the pore space with the limited distance the fluid molecules will move under free diffusion.

The pore properties values used to produce the plots that fit the simulated peak intensities to the experimental are shown in Tables 1, 2, and 3 for Fontainebleau, quartz sand, and Mt. Gambier respectively. The various properties estimated from simulations are radius, r (μm), inter-pore spacing b (μm), exchange time λ (s), inter-pore diffusion coefficient Dp (m^2/s), and tortuosity T . The estimated exchange times between the samples is consistent with their morphology. Both the sand and Mt. Gambier show significant exchange while the Fontainebleau shows very little. Connectivity is known to be typically correlated with porosity; in general, the more porous the material, the better connected the pores are, and therefore more likely that fluid molecules will move between them. In addition, the size of the pores will also determine how quickly molecules move between the different pores. We see this interplay with the exchange times in the sand sample and Mt. Gambier as two samples have similar exchange times. Even though Mt. Gambier is more porous and better connected, it has larger pores. Therefore, though more restricted in their movement, fluid molecules in the sand sample with smaller pores do not need to diffuse as far to move to a new pore.

The sand sample shows general agreement with the tortuosity values from the X-Ray CT analysis, though the exchange between β pores shows a spuriously high tortuosity value. The tortuosity of the Fontainebleau exchange peak is significantly lower than the value found from the X-Ray CT, but considering the uncertainty in the peak intensity due to the low amount of exchange, this is to be expected. The Mt. Gambier shows general agreement with the X-Ray CT results, though the tortuosities found for the cross peaks are on the low side as well.

TABLE 1. Fontainebleau pore properties

r (μm)	$r\alpha$	$b\beta$	
	30	59	
b (μm)	$b\alpha\alpha$	$b\beta\beta$	$b\alpha\beta$
	71	129	90
λ (s)	$\lambda\alpha\alpha$	$\lambda\beta\beta$	$\lambda\alpha\beta$
	1.4	4.5	0.9
Dp (m^2/s)	$D\alpha\alpha$	$D\beta\beta$	$D\alpha\beta$
	5.9×10^{-10}	6.1×10^{-10}	15.0×10^{-10}
T	$T\alpha\alpha$	$T\beta\beta$	$T\alpha\beta$
	3.9	3.8	1.5

TABLE 2. Tight-packed quartz sand pore properties

r (μm)	rα	rβ	rγ			
	16	31	54			
b (μm)	bαα	bββ	bγγ	bαβ	bαγ	bβγ
	35	64	142	39	65	73
λ (s)	λαα	λββ	λγγ	λαβ	λαγ	λβγ
	0.2	1.4	3.9	0.15	0.42	0.51
Dp (m/s²)	Dαα	Dββ	Dγγ	Dαβ	Dαγ	Dβγ
	10.1x10 ⁻¹⁰	4.9x10 ⁻¹⁰	8.51x10 ⁻¹⁰	16.71x10 ⁻¹⁰	16.8x10 ⁻¹⁰	17.3x10 ⁻¹⁰
T	Tαα	Tββ	Tγγ	Tαβ	Tαγ	Tβγ
	2.3	4.7	2.7	1.4	1.4	1.3

TABLE 3. Mt. Gambier pore properties

r (μm)	rα	rβ	rγ			
	17	44	74			
b μm)	bαα	bββ	bγγ	bαβ	bαγ	bβγ
	35	64	142	39	65	73
λ	λαα	λββ	λγγ	λαβ	λαγ	λβγ
	0.2	1.4	3.9	0.15	0.42	0.51
Dp (m/s²)	Dαα	Dββ	Dγγ	Dαβ	Dαγ	Dβγ
	10.1x10 ⁻¹⁰	4.9x10 ⁻¹⁰	8.51x10 ⁻¹⁰	16.71x10 ⁻¹⁰	16.8x10 ⁻¹⁰	17.3x10 ⁻¹⁰
T	Tαα	Tββ	Tγγ	Tαβ	Tαγ	Tβγ
	2.5	2.6	2.5	1.5	1.8	1.7

CONCLUSIONS

The three samples showed exchange behavior consistent with the morphology determined from the X-Ray CT analysis. The very porous Mt. Gambier sample showed the most exchange while the Fontainebleau showed the least. Pore size distributions seem to be consistent with those calculated from X-ray CT, though the propagator resolved method does not manage to capture the full range of inter-pore spacings with diffusion alone. It is conceivable, that the exchange seen is partially due to exchange between narrow regions or the pore space (throats) and more convex larger regions of pore space (pores). While the results are promising, further tests with a larger set of samples is necessary for thorough validation.

ACKNOWLEDGMENTS

The authors would like to acknowledge the Royal Society of New Zealand Marsden Fund, the New Zealand Foundation for Research, Science, and Technology and the Australian Research Council (DP0558185, DP0881112) for financial support. CHA thanks the Australian Research Council for an Australian Research Fellowship.

REFERENCES

1. K. E. Washburn and P.T. Callaghan, *Phys. Rev. Letters* **97**, 175502 (2006).
2. L. Monteilhet, J.P. Korb, J. Mitchell, and P.J. McDonald, *Phys. Rev. E* **74**, 061404 (2006).
3. K.E. Washburn, C.H. Arns, P.T. Callaghan, *Phys. Rev. E* **77**, 051203 (2008).
4. C.H. Arns, A. Sakellariou, T.J. Senden, A.P. Sheppard, R.M. Sok, W.V. Pinczewski, M.A. Knackenstadt, *Petrophysics* **46**, 260-277 (2005).
5. L. Venkataraman, Y.Q. Song, and M.D. Hurlimann, *IEEE Transactions on Signal processing* **50**, 1017 (2002).